Journal of Archaeological Science: Reports, Volume 37, June 2021, Article number 102906
DOI:10.1016/j.jasrep.2021.102906

Assessing the reliability of microbial bioerosion features in burnt bones: A novel approach using feature-labelling in histotaphonomical analysis

Authors

Emese I. VÉGH[1], Andrea CZERMAK[1], Nicholas MÁRQUEZ-GRANT[2] and Rick J. SCHULTING[1]

[1]School of Archaeology, University of Oxford,

[2]Cranfield Forensic Institute, Cranfield University, Defence Academy of the United Kingdom

Corresponding Author: Emese I. Végh, emese.vegh@wolfson.ox.ac.uk, Wolfson College, Linton Road, Oxford, OX2 6UD

Abstract

Objectives: Recent histotaphonomic studies have focused on the presence of features thought to be caused either by bacteria (microscopic focal destruction/MFD and cyanobacterial tunnelling) or fungal (Wedl tunnelling types 1 and 2) attack on unburnt bone. Identifying these characteristics on burnt bones could indicate the state of decomposition before burning, with important repercussions for both archaeological and forensic contexts.

Materials and Methods: Fleshed pig (Sus scrofa, N=25) tibiae were left exposed on a field, then collected at 14-, 34-, 91-, 180-, 365-day intervals before being burnt in an outdoor fire (≤750 °C). Fresh (fleshed) legs (N=10) acted as unburnt and burnt controls. Thin sections were examined using transmitted light microscopy and backscattered scanning electron microscopy. Diagenetic traits were quantitatively and systematically assessed by a novel data labelling application developed for this study.

Results: Features meeting the published characteristics of microbial bioerosion ('Wedl tunnelling', 'lamellate' and 'budded MFD') were significantly correlated with time since deposition on the unburnt bones. The presence of features resembling 'Wedl 2 tunnelling' on fresh burnt bones indicates that they are an artefact. Only budded MFD increased significantly over time in the burnt groups. Features meeting the published characteristics of Wedl 2 tunnelling were present on the fresh burnt bones.

Discussion: The presence of many features seemingly indistinguishable from those caused by bioerosion on the freshly burnt control bones suggests that burning is not only able to conceal features thought to be the result of bioerosion but can produce them as well. Thus, such features are not a reliable indication of bioerosion. Budded MFD may be a viable indicator but more research is required.

Keywords

Microbial bioerosion, burning, bone, cremation, taphonomy

Introduction

Understanding early postmortem changes to the body is of interest in many fields, including archaeology, physical anthropology, forensic science, palaeobiology, and palaeontology. Deciphering early bone diagenesis and shedding light on the processes that lead to fossilisation presents a challenge, one that is further exacerbated when bone is subjected to cremation. Identifying bioerosion on burnt bones would open the possibility of establishing whether a body had gone through a decomposition phase with soft tissue still present prior to burning. This research aims to investigate whether bioerosion features can be used as an indication of decomposition on burnt bones, which has implications to understanding funerary practices in the archaeological record as well as understanding the sequence of events leading to deposition in forensic investigations.

Burning of the body can occur either when the body is fully fleshed (e.g. homicide, suicide, accidental fires, cremation) or once it has decomposed to different degrees (e.g. burning to conceal evidence of murder, cremation, accidental fires, freeing up space in a cemetery) in both archaeological and forensic contexts. Early studies mainly focused on establishing whether bone was at either of the two extremes – fleshed or dry – of the spectrum when burnt (Baby, 1954; Binford, 1963; Buikstra and Swegle, 1989; Etxeberria, 1994; Spennemann and Colley, 1989; Whyte, 2001). The methods employed were primarily macroscopic, recording the presence of warping and of thumbnail fractures (Buikstra & Swegle, 1989; Spennemann & Colley, 1989; Whyte, 2001). However, this has been shown to be relate primarily to collagen content (Gonçalves et al., 2011). Currently, it remains challenging to identify the body's state of decomposition before burning.

A reliable method of establishing the body's stage of decomposition at the point of burning would help determine whether this occurred immediately or sometime after death. In archaeology, the interaction between anthropogenic and natural processes is vital to understand human behaviour connected to past funerary rites. For example, it has been suggested that at some Neolithic and Bronze Age sites in Ireland, including the passage tombs of the Boyne Valley and Fourknocks, as well as Kilgreany cave (Waterman, 1978; Dowd, 2008; Cooney et al. 2014), human remains were either passively or actively excarnated before inhumation and cremation. At other Irish sites, such as Tully, the excavators claimed that the bodies were burnt with full soft tissue coverage (Wells, 1978). These claims were based on supposedly diagnostic fracture patterns, which, as noted above, may be problematic.

There are a few cases discussed in the forensic anthropological literature in which a single individual has been found partially burnt (Bontrager and Nawrocki 2008; Garrido-Varas and Intriago-Leiva 2015). The postmortem intervals were established using both the signs of carnivore gnawing and patterned thermal destruction. However, usually only fragmented calcined remains are encountered. Thus, there is a need for better and more accurate methods of determining the stage of decomposition from a single burnt skeletal fragment.

Bone is a complex, composite material, which undergoes diagenetic alterations post-deposition. Three distinct diagenetic pathways can be distinguished (Collin et al., 2002): (1) chemical degradation of the organic component (collagen hydrolysis); (2) chemical degradation of the inorganic phase (bioapatite dissolution); and (3) microbial degradation of both phases (Child, 1995; Hedges and Millard, 1995; Millard, 2001; Collins et al., 2002; Nielsen-Marsh and Hedges, 2002; Huisman et al., 2017; Turner-Walker and Jans, 2008; Kontopoulos et al., 2016). Pathway 3 presumably happens either (1) rapidly after death as it is thought to be linked to putrefaction processes involving soft tissues (Huisman et al., 2017; Collins et al., 2002; Jans, 2005; Fernández-Jalvo et al., 2010) or (2) by soil bacteria post-deposition (Turner-Walker, 2012, 2019; Kendall et al. 2018). This study focuses on this pathway's (i.e. microbial degradation) supposedly diagnostic features in an effort to shed light on the early postmortem history of the remains.

Histotaphonomy, the taphonomy of bone at the microstructural level, has been often employed by researchers to investigate the biological deterioration of bone (e.g. White and Booth, 2014; Kontopoulos et al., 2016). Many studies use features of bacterial attack on unburnt bones to inform on the initial postmortem period of the body (Child, 1995; Jans et al., 2004; Nielsen-Marsh, et al., 2007; Hollund, et al., 2012; Hollund, et al., 2014; White and Booth, 2014). Whether the origin of the bioerosive bacteria is endogenous or exogenous, most studies focus on archaeological bone (Jans et al., 2002; Turner-Walker and Jans 2008; Brönnimann et al., 2018), and some on recent bone (Yoshino, et al., 1991; White and Booth, 2014; Kontopoulos et al., 2016; Lemmers et al., 2020). Furthermore, to our knowledge there have only been two studies on histotaphonomic features on burnt bones (Grévin et al., 1991; Lemmers et al., 2020). Grévin et al., (1991) reported that human bones from a Late Bronze Age site at Pincevent, France, had been buried for weeks to months prior to cremation based on microradiographs showing 'typical' postmortem bacterial attack. Recently, Lemmers et al., (2020) proposed that bioerosion features survive in burnt bones and can be readily distinguished from alterations in the microstructure caused by burning.

All scholarship agrees that there is a need for more experimental histological studies. This paper aims to assess whether bioerosion features are useful indicators of decomposition in burnt bones.

1.1 Histotaphonomic features in bone

The specific causative agents of microstructural changes are poorly known, but mainly they are attributed to bacteria, fungi, or marine based organisms (Bell, 2012a). Microbiological decay of the body commences soon after death. Bacteria and fungi alter hard tissues by entering through bone's vasculature (Bell et al., 1996; Millard, 2001). The bacterial flora in the gut initially affect the bone from the endosteal surface, while exogenous bacteria from the environment (e.g. soil) attack the bone from the periosteal surface (Hackett, 1981; Jans, 2008; Daniel and Chin 2010; Boaks et al., 2014; White and Booth, 2014; Kontopoulos et al., 2016).

Morphological changes to bone resulting from bioerosion was first described by Wedl (1864) and Roux (1887), and subsequently by Hackett (1981) and Garland (1987). These changes include (1) small channels (Wedl, 1864) caused by fungi (Roux, 1887), (2) microscopic focal destruction (MFD), which can be linear longitudinal, lamellate, or budded (Hackett, 1981), and (3) other types of diagenetic changes, such as reduction in birefringence, inclusions, and infiltrations (Garland, 1987). Hedges, Millard, and Pike (1995) developed the *Oxford Histological Index* (OHI) to approximate the preservation of bone histology. The OHI is still used in bone histology studies, providing an ordinal scale assessment of the degree to which bone is affected by bioerosion. We build on this here by including a quantitative assessment of the percentage of the bone affected.

More recent research has focused mainly on the presence of MFD, Wedl tunnelling, Wedl type 2, and cyanobacterial tunnelling on unburnt bone (see Table 1).

Feature	Appearance	Causative agent	Context and Environment
Microscopic Focal Destruction (MFD)	Linear, Budded, or Lamellate structures around Haversian canals	Endogenous bacteria (Bell et al., 1996; Jans et al., 2004; Jans, 2013; Nielsen-Marsh et al., 2007; Trueman and Martill, 2002; White and Booth 2014)	Terrestrial
		Soil bacteria (Turner-Walker, 2014; Grine et al., 2015; Kontopoulos et al., 2016; Kendall et al., 2018; Morales et al., 2018)	

Wedl tunnelling	Dendritic structures	Fungi (Hackett, 1981; Bell et al., 1991; Trueman and Martill, 2002)	Marine (Garland, 1987; Millard, 1993)
			Terrestrial: surface exposed and/or buried de-fleshed bones (Trueman and Martill, 2002; Jans, 2008; Brönnimann et al., 2018)
			Oxygenated, wet environments in neutral to acidic soils (Huisman et al., 2009, 2017)
Wedl type 2/Enlarged canaliculi/enlarged osteocyte lacunae/Non-Wedl MFD	Enlarged canaliculi, resembling a spider-like structure	Fungi (Trueman and Martill, 2002; Kontopoulos et al., 2016; Kontopoulos, 2019)	Terrestrial
		Bacteria (White and Booth, 2014; Booth, 2016)	
Cyanobacterial tunnelling	Tunnelling from periosteal surface of bone	Bacteria (Bell et al., 1991; Jans, 2008; Bell, 2012a; Turner-Walker, 2012, Turner-Walker 2014)	Marine- or fresh water (Bell et al., 1991; Jans 2008; Bell, 2012a; Turner-Walker, 2012, Turner-Walker, 2014)

Table 1. Microbial bioerosion features, their thought to be causative agents, contexts and environments in the literature.

Diagenetic features on bones are usually studied under either transmitted light microscopy (Jans et al., 2002; Jans et al., 2004; Jans 2005; Tjelldén et al., 2018) or electron microscopy (Bell et al., 1991; Bell, 2012b; Turner-Walker, 2014), with a few studies employing both methods (Huisman et al., 2017; Turner-Walker 2019). General changes in bone microstructure due to bacterial attack manifest in demineralised (darker) and adjacent hypermineralised (brighter) areas on the backscattered scanning electron microscope (BSEM), which recently has been proposed to be a more effective means of identifying bioerosion features (Turner-Walker 2019).

Complicating discussion of histotaphonomical features is the fact that morphologically identical or similar features have been given different terms in the literature (see Table 2). For example, the same dendritic features often called Wedl tunnels (Brönnimann, et al., 2018), are also called as non-Wedl MFD (Fernández-Jalvo et al., 2010), Wedl type 2 (Trueman and Martill, 2002; Brönnimann et al., 2018), lichen penetration (Fernández-Jalvo et al., 2010), and early stage of non-Wedl MFD (White and Booth, 2014). This distinction is crucial, since for example Wedl tunnelling are thought to be caused by fungi from the burial environment (Fernández-Jalvo et al., 2010; Brönnimann et al., 2018), while non-Wedl MFD have been

attributed to bacterial activity, most often from the gut (Bell et al., 1996; Jans et al., 2004; Jans, 2013; Nielsen-Marsh et al., 2007; Trueman and Martill, 2002; White and Booth, 2014). The present study uses the terminology outlined by Brönnimann et al. (2018) because of its clear illustrations and descriptions.

Table 2
Identical histotaphonomic features named differently across the literature.

Feature	Different naming of the features across the literature			
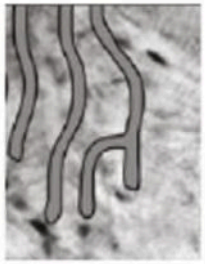	 Cyanobacterial tunnelling, (Huisman et al., 2017, 20, Fig 4.A)	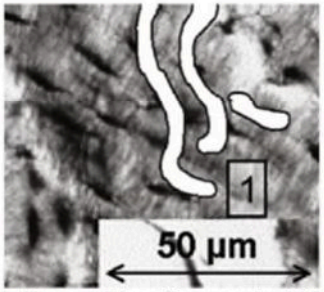 Wedl tunnelling (Jans et al., 2004, 89, Fig 1)	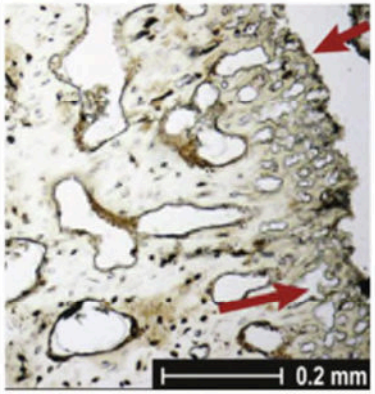 Cyanobacterial tunnelling (Brönnimann et al., 2018, 50, Fig 4G)	 Wedl tunnelling – no scale provided, x170 (Hackett, 1981, 251, Fig 2)
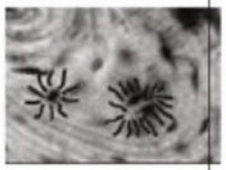	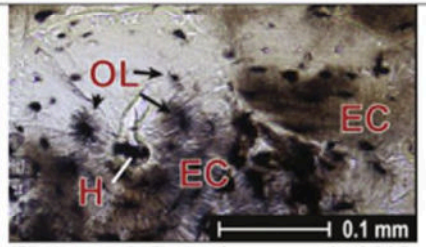 Wedl type 2 (Brönnimann et al., 2018, 50, Fig 4E)	 Expanded osteocytic lacunae and canaliculi due to environmental infiltration (Tjelldén et al. 2018, 412, Fig. 6)	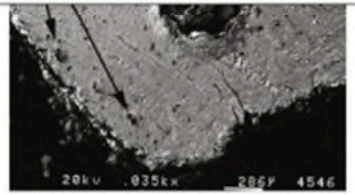 Lichen penetration (Fernández-Jalvo et al., 2010, 74, Fig 7.4)	

1.2 Histology of burnt bone

The primary focus of burnt bone histology studies has been on estimating fire temperature and duration (Herrmann, 1976, 1977; Nicholson, 1993; Holden et al., 1995a,b; Quatrehomme et al., 1998; Ubelaker, 2009; Absolonova et al., 2013; Imaizumi et al., 2014; Cambra-Moo et al., 2017) or on species identification (Cattaneo et al., 1999) using histomorphometry or histomorphology (Table 3). There is a considerable disagreement between different authors on when, and if, identifiable histological changes take place. The histological structure of bone has been variously reported to be nearly identical to that of unburnt bone when burnt under 600°C (Bradtmiller and Buikstra, 1984), 700°C (Herrmann, 1977), 900°C (Squires et al., 2011), or 1200°C (Cattaneo et al., 1999). However, it is unknown whether these were bone or air temperatures, which might be a source of discrepancy. Other complicating factors include the method of burning (e.g., furnace or natural fire), the type, size, and state of the bone, and the presence/absence of soft tissues.

Investigating histomorphological changes due to burning are essential to the current study, because these can influence the appearance of microbial bioerosion and hence their recognition to identify the postmortem stage at which the bones were burnt.

Temperature (°C)	**Histomorphometric Changes**	**Histomorphology Changes**
500	Increase in size and number of cracks due to differential shrinkage of bone tissues (Imaizumi et al., 2014)	Cracking, minute fissures, separation of the osteons from interstitial lamellae (Imaizumi et al., 2014)
<600	No change, identical to unburnt bones (Absolonova et al., 2013) No cracking with minimal carbon deposits (Hanson and Cain, 2007) Microfeatures identifiable, but less well preserved (Caroll and Squires, 2020)	
600	Increase in osteon size diameter (Bradtmiller and Buikstra, 1984)	Individual lamellae often indistinguishable (Nelson, 1992) Histological structures disappear with extensive carbon deposits (Hanson and Cain, 2007)
	Haversian canals increased in size while the osteon's diameter decreased (Nelson, 1992)	
<700	No change, identical to unburnt bones (Herrmann, 1976, 1977) Cracks present outwards of vascular canals (Hanson and Cain 2007)	
700-800	Structural changes occur (Herrmann, 1976, 1977; Hummel and Schutkowski, 1987; Absolonova et al., 2013)	
800	No changes below, shrinkage above (Van Vark, 1970)	No major changes below (Van Vark, 1970)
	No significant shrinkage (Cattaneo et al., 1999)	Lamellar structure of bone is lost (Holden et al., 1995b)

900	Microstructural changes occur (Squires et al., 2011)	Haversian and Volkmann's canals cannot be distinguished, no microstructure preserved (Squires et al., 2011) Granular surface appears (Castillo et al., 2013) 700-900 °C: Degeneration of microscopic structures (<60% of area, Carroll and Squires, 2020)
1000	Shrinkage occurs (Cattaneo et al., 1999)	Haversian canals survive, while Volkmann's canals, circumferential lamellae, resorption cavities are hard to differentiate (Absolonova et al., 2013) Few misshapen Haversian canals survive, but 86.3% of sample area show complete fusion of hydroxyapatite (Caroll and Squires, 2020)
1200	Microstructural changes start to occur (Cattaneo et al., 1999)	
1400		Haversian Canals and osteocyte lacunae indistinguishable (Holden et al., 1995b)
1600	All structural features are completely destroyed (Holden et al., 1995b; Fairgrieve, 2008)	

Table 3. Histomorphometric and histomorphology changes of burnt bone in the literature.

Materials and Methods

2.1 Experiment

Fleshed *Sus scrofa domesticus* (pig) tibiae were sourced from a local butcher, euthanised at 18 months. All limbs were kept in a freezer at –18°C until collection. Pigs, in addition to being easily sourced, have been widely utilised as a substitute for human bodies in decomposition, fire, and histology studies (Forbes et al., 2005; Lynn and Fairgrieve, 2009; Thompson and Inglis, 2009; Bonney et al., 2011; Symes et al., 2012; White and Booth 2014; Kontopoulos et al., 2016). There is an ongoing discussion on how appropriate pigs are as human analogues (Matuszewski et al. 2020), but they are considered to be reasonable proxies in many respects, including bone macro- and microstructure, remodelling, mineral concentration and density, as well as gut microbiota (Turner and Wiltshire, 1999; Forbes et al., 2005; Pearce et al., 2007; Wilson et al., 2007; Feng and Jasiuk, 2011; Hollund et al., 2014; White and Booth, 2014; Kontopoulos et al., 2016). Long bones were chosen for the

200 study because of their common use in histological studies, their large cortical bone area, and
201 their survival rate (Booth and Madgwick, 2016).

202 The pig tibiae (N=25) were left to decay for 14, 34, 91, 180, and 365 days prior to
203 burning on an outdoor fire. Fresh fleshed bones (N=10) served as unburnt and burnt control
204 samples. The first round of fleshed tibiae were sub-aerially deposited on an open grassland
205 area at Wytham Woods, Oxfordshire, England, in June 2018 and between February and June
206 2019. The exposed tibiae were protected from scavengers with a cage covered by layers of
207 iron mesh. Scavenging produced tooth marks on nearly all bones, but only a few bones were
208 completely removed from the cage (one of the 180-day and four of the 365-day postmortem
209 bones).

210 Wytham Woods is located in a temperate climate with moderate to high rainfall
211 averaging 717 mm, with monthly mean temperatures ranging from 1.6 °C in January to 20.3
212 °C in July with a long-term annual mean of 10.0 °C (Taylor et al., 2011). At collection bones
213 were partially covered by the soil, which may have instigated exogenous bioerosion. Soil pH
214 range from 3 to 7 (Taylor et al., 2011).

Fig. 1. Burning of the 14- and 34-day postmortem bones on the pyre. Upper image was taken subsequently after the ignition of the fire, while the lower was taken when the bones have calcined. All outdoor fires were executed in the same manner. The pyres were

built on a flat clearing, using bricks to provide support for a wire mesh holding the bones, as well as partial protection from the wind. While offering less control over temperature rather than a furnace, the use of an outdoor fire better reflects real-world conditions due to the more variable temperatures of the fire, and the influence of the wind. Each fire was built and maintained in the same manner, using a mixture of hard and soft woods as fuel.

Pyres were built and maintained in the same manner (Fig. 1), each fire lasting 2.5-3 hours, until the bones calcined (Fig. 1). Bone temperatures were monitored by a thermocouple, averaging 553 °C, with a recorded maximum of 751 °C. Maximum fire temperatures reached 995 °C. The bones were left to cool and subsequently collected for transport.

2.2 Analysis

Unburnt samples were defatted in a 2:1 chloroform:methanol mixture for between 8 and 20 weeks, in order to remove fat infilling the pores of bone tissues. Samples were taken before and after burning from the minimum diameter of the tibiae diaphyses. Samples were embedded undecalcified in transparent epoxy cold mounting resin and a catalyst (Spectrographic Ltd., Leeds, UK), in order to impregnate the bones within a solid medium to facilitate sectioning for microscopical analysis (Garland, 1987). The resin blocks (N=56) were then placed into a desiccator with vacuum pump to inhibit bubble formation. Two transverse thin sections (~50-70 μm) were cut from each sample using a Buehler saw fitted with a diamond blade (Buehler, Lake Bluff, IL, USA) and subsequently fixed onto glass slides using Eukitt mounting medium (Merck, Darmstadt, Germany) and covered with microscope glass slides.

The slides were examined under a Leica DM 2500 P transmission light microscopy with (Leica, Wetzlar, Germany) using normal and polarised light at 50x, 100x, and 400x magnification. Each sample was composed of three to five images, which were taken across the bone with a USB camera (Brunel Microscopes Ltd., Chippenham, UK) per thin section at 50x magnification to represent bone from the periosteal to the endosteal surfaces, through the mid-cortical region for quantitative analysis. Higher magnification images were taken to observe and document more closely the features of interest.

Diagenetic traits on the optical microscopy images (N=270) were quantitatively assessed by calculating the percentage of areas affected by diagenetic and/or heat-induced features. This was done by a human observer clicking on the features present on each block (N=27,000) of randomly selected images in a data labelling application built for this study in Python (Flask web framework) and Javascript (jQuery library) programming languages. Each image (at 50x magnification) was divided into 100 equal blocks. The random selection of images across all samples by the application excluded bias in labelling, hence the samples were examined 'blind'. Results were automatically saved into a database recording whether a feature was present or absent within a block. The cumulative score of the 100 blocks estimates the proportion of the initial image that contains a given feature. Features (Fig 2) were labelled according to descriptions in Brönnimann et al. (2018, 46, Fig. 1), which are in turn based on figures in Jans (2004, 89, Fig. 1) and Hackett (1981, 250, Fig. 1). Features were initially labelled according to their closest comparanda in the literature, with no presuppositions being made regarding the veracity of the labels. This usage is indicated by single quotation marks. Some features were more variable in appearance than those discussed in the literature. For example, the label 'cyanobacterial tunnelling' was applied when the tunnels looked the most like the image in Brönnimann et al. (2018) taking into account tunnel diameters (Fig. 3) after re-examination of all images by the same researcher (EIV).

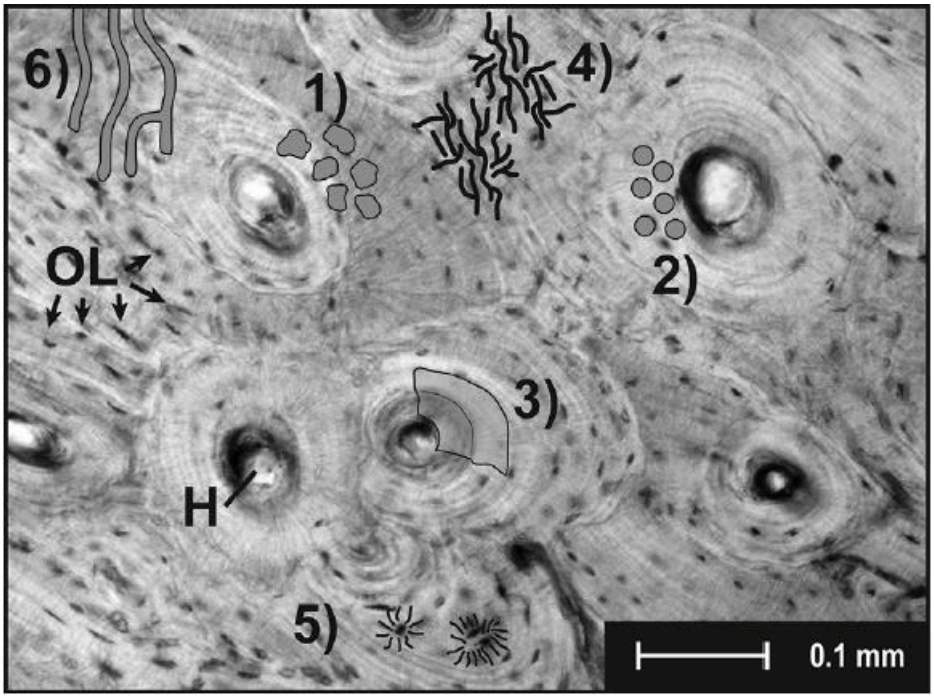

Fig. 2. Criteria for labelling microbial bioerosion from Brönnimann et al., 2018. 1) Budded MFD; 2) Linear longitudinal MFD; 3) Lamellate MFD; 4) Wedl tunnelling; 5) Wedl

2; 6) Cyanobacterial tunnelling (Brönnimann et al., 2018, 46, Fig. 4). Features that appeared to be similar to linear MFD were not labelled in this study, because they were caused by burning.

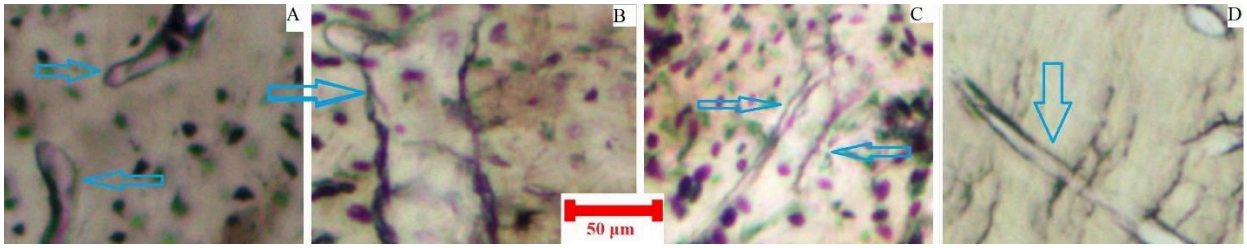

Fig. 3. Variation of features appearing to be tunnels in the different samples. ***A*** *and* ***B*** *are of Volkmann's canals,* ***C*** *and* ***D*** *are unidentified channels and hence were labelled having the appearance of features consistent with 'cyanobacterial tunnelling', even though there is no clear indication of cyanobacteria being present in a terrestrial context, and the tunnel in* ***D*** *appears to be connected to a Haversian canal. The features are indicated by the blue arrows. Note the differences in the width of the tunnels. In the literature, maximum tunnel diameters caused by microorganisms have been reported to be between 0.1 and 2.0 micron (terrestrial), 7-18 microns (freshwater), and 5-19 microns (marine, Pesquero* et al.*, 2018). Here, diameters under 20 microns were considered to be 'cyanobacterial tunnelling', while >20 microns were classed as Volkmann's canals. (Transmitted light microscopy, 50x, from left to right: WSF2D2W5_unburnt, WSF2D2W5_burnt, WSF1D1M2_unburnt, WSF1D1M2_burnt).*

The prevalence of features on unburnt and burnt bones was then statistically analysed using Jupyter notebook in Python programming language (Pandas, Matplotlib, Seaborn, SciPy, and Numpy libraries). Linear regression was used to measure the strength of the relationship between the presence (in percentage) of each taphonomic feature and the length of the postmortem period before and after burning, with statistical significance assessed by associated p-values ($\alpha = 0.05$). The null hypothesis was that the presence (in %) of a given feature per bone does not increase with the postmortem interval. The coefficient of variation (CV) was used to assess the dispersion of the features in different decompositional stages and burning status.

Validation of whether or not features were due to bioerosion was then undertaken using a BSEM detector in the electron microprobe. The contrast on the images resulting from demineralised and hypermineralised areas can be used to identify bioerosion (Turner-Walker, 2019). The resin blocks were ground with carborundum paper of progressively finer grit size (800, 1200, 2500). The blocks were then polished on a Buehler wheel and a satin woven acetate polishing cloth (DP-Dac, Struers A/S) using 3 μm and 1 μm monocrystalline diamond paste and suspension (DP-Paste M, Struers A/S and MetaDi, Buehler, respectively) for 30 and 5 minutes, respectively. The mounts were cleaned in an ultra-sonic bath in petroleum ether (40°-60°C). Samples were carbon-coated using a carbon evaporation coater (HHV Auto 360), the carbon acting as a conductive layer to prevent charging.

Results

The percentage of given features present for each decompositional stage before and after burning is shown in Fig. 3. The most common taphonomic features affecting the largest percentage of the bone areas were hairline cracks and those similar to what has been described in the literature as 'Wedl type 2'. The latter feature was absent from the unburnt fresh/control group but was present on the freshly burnt controls. 'Wedl 2' was also present after only 2 weeks of deposition on both the unburnt (26.32%) and burnt (26.43%) groups. After 1 year, this feature was present on over half of the areas investigated (53.5%).

The unburnt control group presented a very small number of 'Wedl tunnelling' (0.75%), 'Wedl 2' (0.75%), 'lamellate' (0.25%) and 'budded MFD' (0.50%) and tunnels resembling 'cyanobacterial tunnelling' (3.5%). These are attributed to human labelling errors, and quantify labelling error, which is negligible for almost all categories, due to the impossibility of bioerosion being present on the control bones. As cyanobacterial tunnelling cannot be present on these bones, they are almost certainly mislabelled Volkmann's canals. Hairline cracks are abundant on this group (22.5%). This group should not show any sign of microbial bioerosion, since the pigs were dismembered shortly after death and were not exposed to soil. Conversely, the burnt fresh/control group exhibited significantly higher percentages of features consistence with 'Wedl tunnelling' (4.25%), 'Wedl 2' (11.68%) and tunnels resembling 'cyanobacterial tunnelling' (7.56%) as identified in the literature.

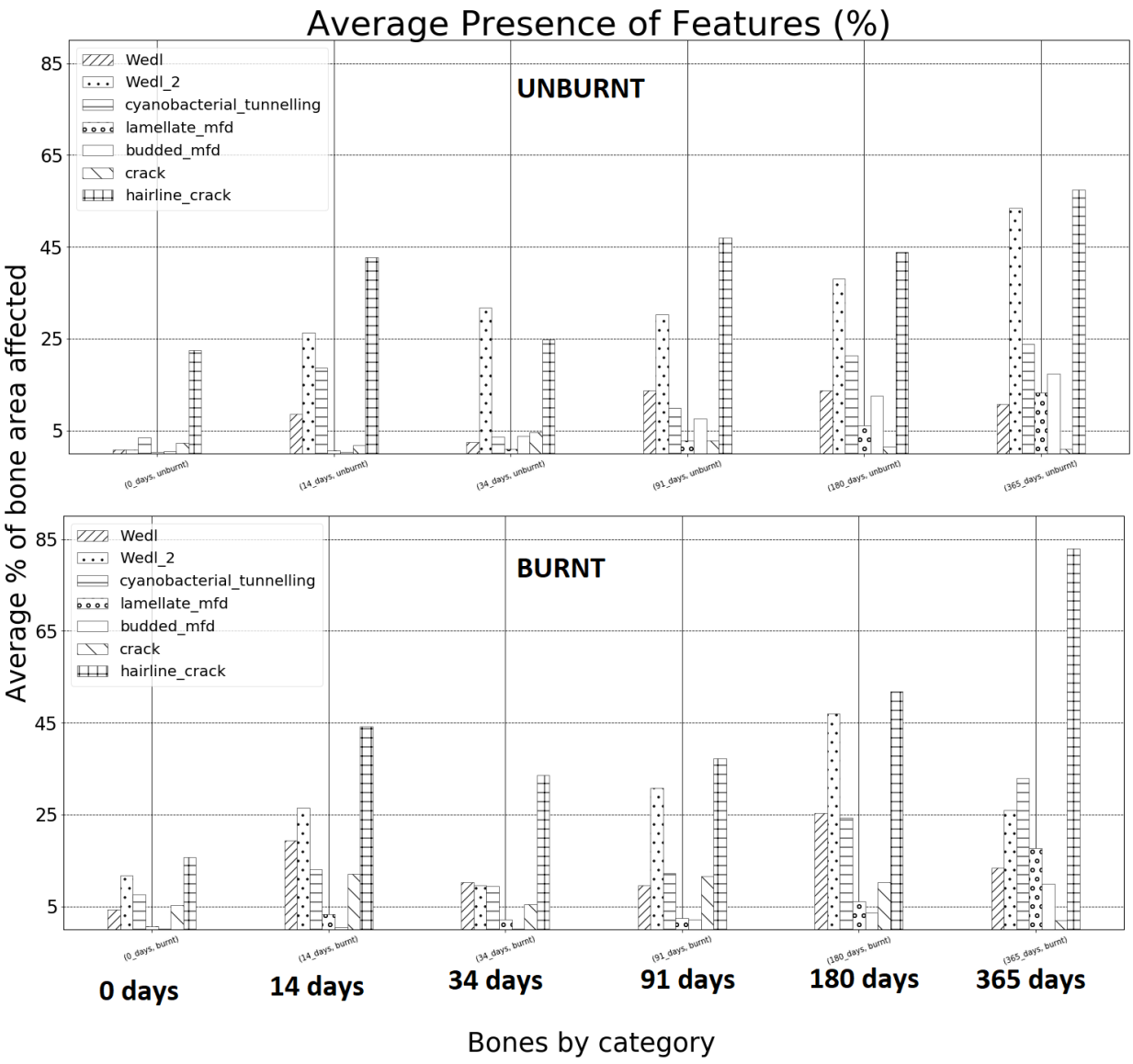

Fig. 4. The average presence of the taphonomic features at each stage of decomposition before (upper) and after (lower) burning.

Diagenetic features increase for all bone categories after burning in all decompositional stages. There was a moderate positive linear correlation between time passed since deposition and percentage of the presence of 'Wedl tunnelling' ($r=0.442$, $p<0.0001$), 'lamellate MFD' ($r=0.493$, $p<0.001$), 'budded MFD' ($r=0.531$, $p<0.001$) on the unburnt bones, while hairline cracks ($r=0.278$, $p<0.017$), showed a weaker correlation with time, though it remained significant (Table 4). Weak but significant correlations were observed for 'Wedl 2' ($r=0.254$, $p<0.012$) and 'budded MFD' ($r=0.296$, $p<0.006$) in burnt bones.

Feature	r unburnt	p unburnt	r burnt	p burnt
Wedl tunnelling	0.442	0.00009**	-0.016	0.886
Wedl 2	0.170	0.151	0.254	0.012**
Cyanobacterial tunnelling	-0.204	0.084	0.114	0.312
Lamellate mfd	0.493	0.00001**	0.091	0.412
Budded mfd	0.531	0.000001**	0.296	0.006**
Crack	0.064	0.591	0.184	0.095
Hairline crack	0.278	0.017**	0.159	0.150

*Table 4. Correlation Coefficient ('r') and p-value ('p') for each analysed feature on the unburnt and burnt bones. H_0= Presence (in %) of X feature per bone does not increase with postmortem time period. ** indicates significant p-values.*

The coefficient of variation (CV) shows that hairline cracks had the lowest variability between samples of the same decompositional stage (Table 5), while 'lamellate' and 'budded MFD' showed the greatest variability. In general, features were less variable pre-burning than post-burning. The 91 days unburnt, 180 and 365 days postmortem unburnt and burnt bones had the lowest CV scores across all features. The 14-day burnt bones with features recalling 'budded MFD' (2.73) showed the highest variability.

Coefficient of Variation (CV)								
Bones		**Wedl**	**Wedl_2**	**Cyanobacterial tunnelling**	**Lamellate MFD**	**Budded MFD**	**Cracks**	**Hairline cracks**
0 days	unburnt	1.27	0.66	0.82	2.00	1.15	0.75	0.50
	burnt	1.37	1.71	1.00	1.83	2.73	0.89	1.18
14 days	unburnt	0.72	0.52	0.56	1.36	2.07	1.82	0.30
	burnt	1.15	0.94	0.63	1.00	4.00	0.68	0.61
34 days	unburnt	1.24	0.64	0.73	1.10	1.33	0.94	0.60
	burnt	0.80	1.05	0.71	1.73	2.07	0.74	0.57
91 days	unburnt	0.49	0.70	0.60	0.95	0.98	1.20	0.24
	burnt	1.22	0.94	1.16	1.37	2.21	1.10	0.78
180 days	unburnt	0.43	0.64	0.40	0.55	0.67	1.40	0.31
	burnt	0.93	0.35	0.45	0.87	0.60	0.79	0.45
365 days	unburnt	0.80	0.51	0.36	0.25	0.50	2.00	0.27
	burnt	0.60	0.78	0.50	0.11	0.26	1.00	0.02

348 *Table. 5. Coefficients of variation for each feature on the grouped samples by postmortem*
349 *period and state of burning.*

350 The BSEM images (Table 6) present bioerosion-like hypermineralised 'tunnels',
351 which are due to heavy mineral loading in growing individuals (Fig. 5), and thus not the
352 result of bioerosion. A small number of images indicate initial stages of bacterial attack on
353 some of the exposed unburnt bones, for instance one of the 3-months exposed unburnt bones
354 (Fig. 6). Bioerosion was not present on any of the burnt samples. Generally, contrast varied
355 across the burnt bones, while there was no significant difference across the unburnt bones.

Decompositional stage	**State**	**Contrast difference present? (trabecular, mid-cortical, periosteal)**	**Tunnels/cracks with hypermineralised rims?**
Fresh	unburnt	No	No
Fresh	burnt	Yes	No
2 weeks	unburnt	No	No
2 weeks	burnt	Yes	Not generally, except 1
1 month	unburnt	No	Yes
1 month	burnt	No	No
3 months	unburnt	No	Yes, around tunnels/cracks and Wedl 2/MFD
3 months	burnt	Yes	No
6 months	unburnt	No	No
6 months	burnt	Yes	No
12 months	unburnt	No	No
12 months	burnt	Yes	No, but grey colour around tunnels

356 *Table 6. Analysis of compositional images.*

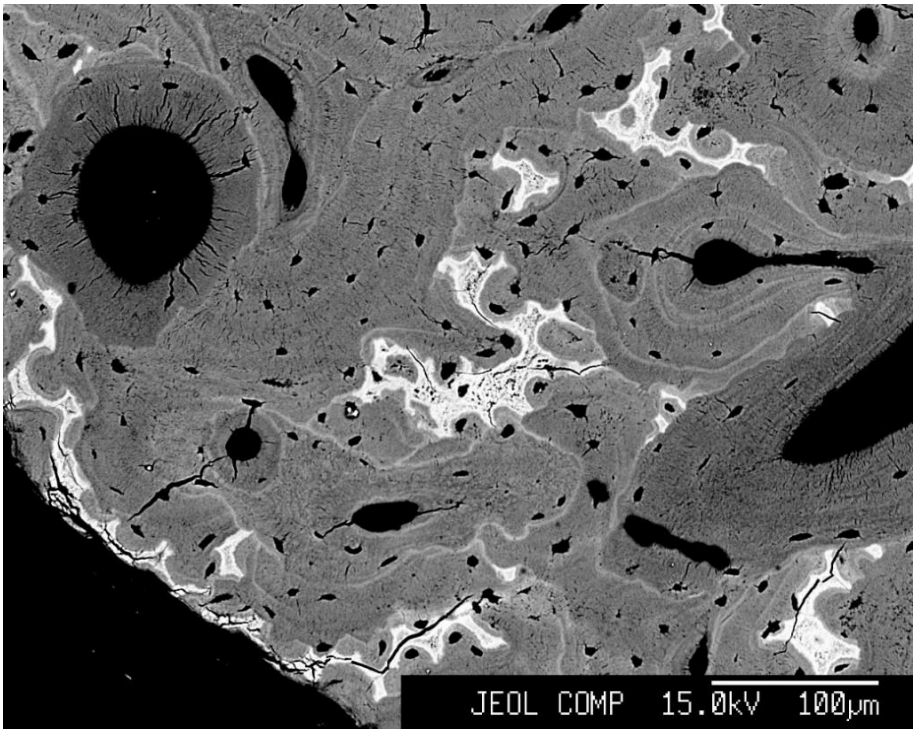

Fig. 5. Backscattered electron image of one of the 1-month postmortem unburnt bones (WSF5D1M3_unburnt). Note the brighter (hypermineralised) areas around the black (demineralised) 'tunnels' toward the lower end of the image. These bright areas are in fact not due to bioerosion, but to heavy mineral loading in growing individuals where osteonal bone has not replaced the primary lamellar bone.

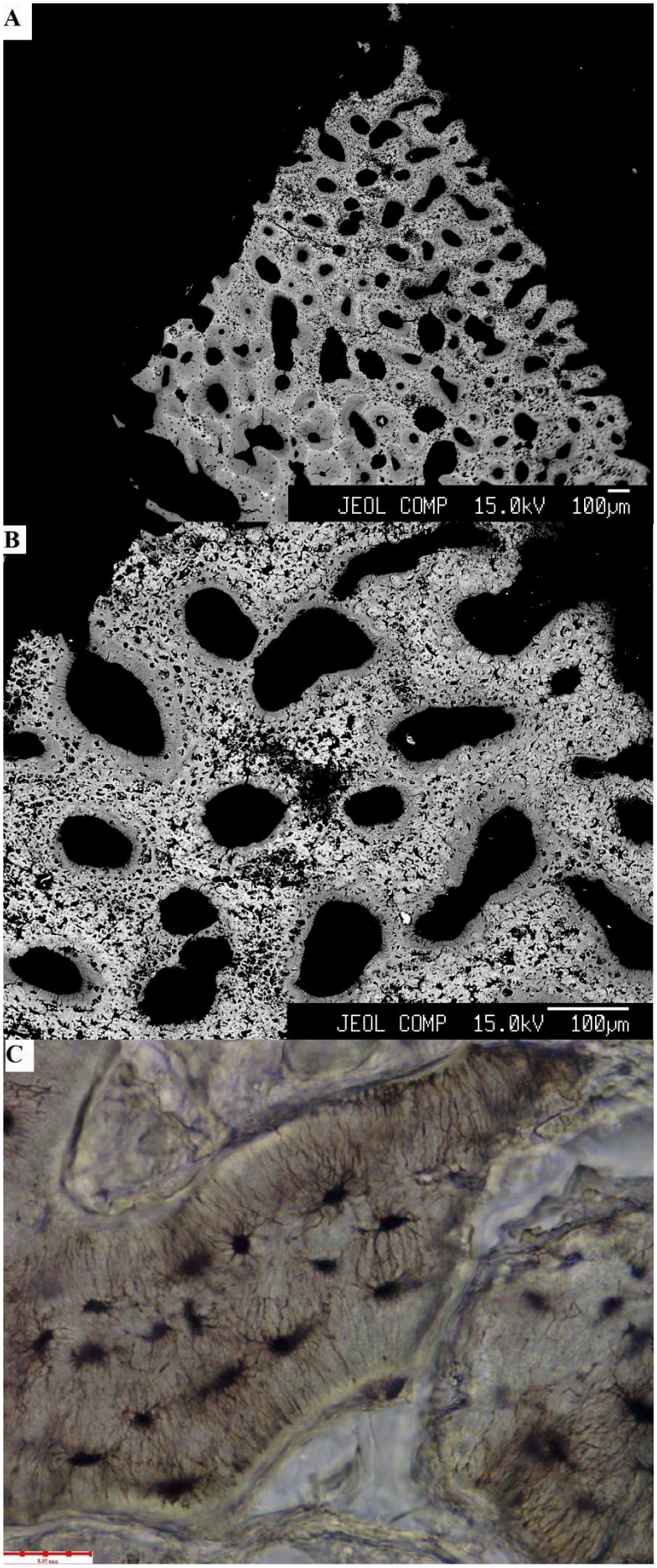

363

*Fig. 6**A** and **B:** Backscattered electron image of 3-month postmortem unburnt bone (WSF3D3M3_unburnt). Note the accumulation of darker (demineralised) circular areas (appearing to be 'Wedl 2' or enlarged canaliculi, but probably naturally demineralised primary bone with microcracks) with bright (hypermineralised) areas around. **C:** Transmitted light microscopy image of a thin section from the same sample (WSF3D3M3_unburnt) at 400x magnification.*

Discussion

Three features associated in the literature with microbial bioerosion are present on the burnt fresh/control group but absent on the fresh unburnt group. The clear implication is that, despite their apparent similarity, these are not bioerosional features but are instead artefacts induced by burning. The feature labelled as 'Wedl type 2' appears on 11.68% of the areas affected on the burnt fresh/control bones (Fig. 7). The frequency of 'Wedl 2' shows a statistically significant relationship with postmortem time interval only in the burnt samples. This feature has been alternatively interpreted as an indication of bioerosion caused by fungi (Trueman and Martill, 2002), but the aetiology of enlarged lacunae and canaliculi is uncertain and has also been associated with staining, mineral infiltration, and burning (White and Booth, 2014; Hanson and Cain 2017). Supporting this, it was found there that these are in fact carbonised osteocyte cells trapped in the canaliculi due to burning (Fig 8.). This observation challenges the interpretation of the cremated remains reported by Grévin et al. (1991), where researchers noted these enlarged canaliculi (referred to here as 'Wedl 2') to be the sign of a delay of weeks to months before cremation. The high variance (CV=1.71) of 'Wedl 2' presence on the freshly burnt samples further suggests that the feature was produced by fire.

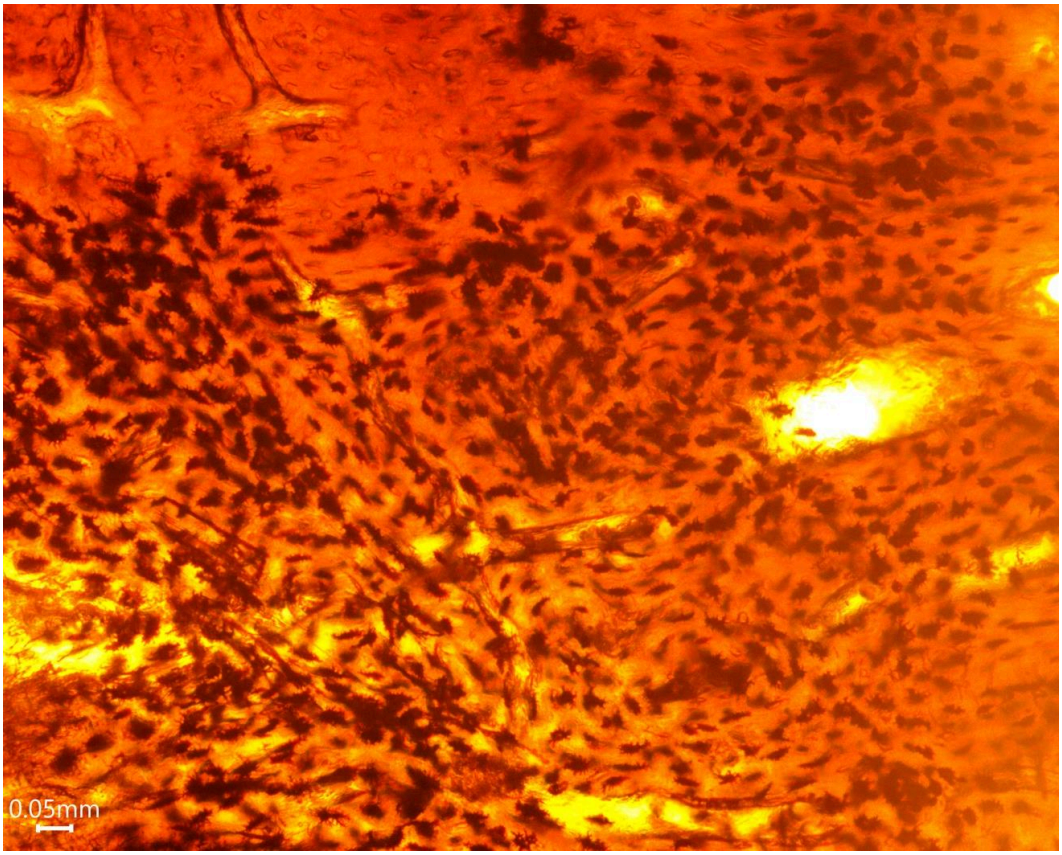

Fig. 7. Staining of the osteocyte-canalicular network that appears to be Wedl type 2 on one of the fresh burnt control bones (SWF1FR2_burnt_1). The tunnels were labelled 'blind' as 'cyanobacterial tunnelling', but these are Volkmann's canals. Neither of these features should be present on freshly burnt bones. Transmission light microscopy, 100x magnification.

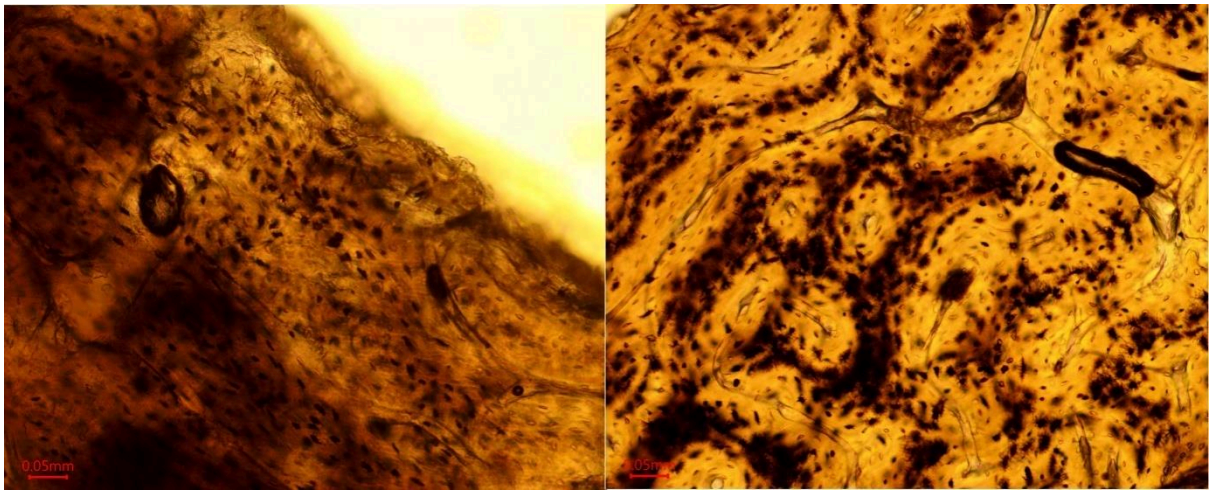

Fig. 8. Staining that appears to be 'Wedl 2'. While it is restricted to some canaliculi on the unburnt 6-months postmortem section (left), it affects all osteons on the same burnt

bone (right). 'Wedl type 2' features are probably due to discolouration on the freshly burnt bones. The source of discolouration can be: (1) sooting from combustion gasses infiltrating the osteocyte-canalicular network after most of the organic matter has burnt out; or (2) iron, manganese, or other metal ions infiltrating the osteocyte-canalicular network prior to burning and then reduced to darker species, such as manganese dioxide or magnetite, when the bones were burnt. While the pig tibiae were not buried, those that were exposed for sufficiently long did become partly covered in soil, which may have presented the opportunity for the infiltration of metal ions. (Sample WSF5D6M1_1, transmission light microscopy, 100x magnification).

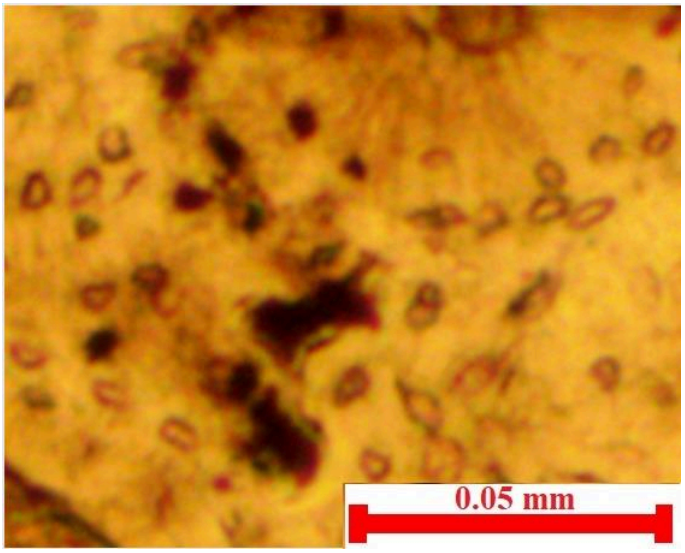

Fig. 9. Features resembling 'budded MFD' from a 6-months postmortem burnt bone (WSF5D6M3_burnt). Transmitted light microscopy, 50x

The frequency of features labelled as 'Wedl tunnelling', and 'lamellate MFD' increase significantly with decay time on unburnt bones, and although they were present, they showed no correlation with time since deposition in the burnt groups. Wedl tunnelling is thought to be attributed to surface exposed and/or buried de-fleshed bones from terrestrial environments (Trueman and Martill, 2002; Jans, 2008; Brönnimann et al., 2018) and should only happen in oxygenated wet environments in neutral to acidic soils (Huisman et al., 2009, 2017). Most bones were covered by soft tissue to different degrees. Less soft tissue coverage means bone desiccation begins earlier, which might limit the intensity of bioerosion (Jans et al., 2004; Nielsen-Marsh et al., 2007). Although the 1-month postmortem unburnt bones were much less affected by 'Wedl tunnelling', the other groups with soft tissues were more affected by

this feature. Therefore, no difference was found in bones with remnants of soft tissues and de-fleshed (by scavenging) bones in the mean bone areas affected by 'Wedl tunnelling'. Sub-aerial exposure, the water-logged soil, and the pH (3-7; Farmer, 1995) suggest Wedl tunnelling should be present (Huisman et al., 2009, 2017), but the fact that it was more frequent in the burnt than in the unburnt bones suggests that similar features are not due to fungal activity and can be produced by burning.

Although the literature suggests that MFD might indicate an endogenous source of bacteria, here it can be ruled out. 'Budded MFD' was the only feature to consistently show a statistically significant correlation with time since deposition for both the unburnt and burnt groups. Post-burning this relationship becomes less robust, suggesting that these features are more likely to be lost or at least become less visible through burning. In addition, this was the least reliably present on all bones, followed by 'lamellate MFD'. 'Budded MFD' (Fig. 9) appeared on the unburnt bones after just 34 days, but it was rarely observed on the same burnt group (0.19%), increasing slightly in the 3-month postmortem group (2.14%). Its presence reaches 10% after a year of decomposition post-burning, suggesting that 'budded MFD' can also be produced by burning.

If bone colonization by microorganism occurs and manifests as budded MFD, it must happen before burning, because this destroys the organic component on which bacteria feed (Grévin et al., 1991). The seasonality of functional activity of microbial communities associated with putrefaction has been investigated (Pechal et al., 2013). It was noted that the carbon consumption of bacterial communities in bone was the highest in Spring, when the 1- and 3-month postmortem bones were placed in the cage. The appearance of budded MFD after just 1-month postmortem would conventionally be attributed to endogenous bacteria that spread through the bone's vasculature causing bioerosion; however, since the pigs were dismembered shortly after death and frozen until they were deposited in the cages, endogenous bacteria as a source can be excluded. Although time is thought to be the least important factor in bioerosion (Piepenbrink, 1986; Piepenbrink and Schutkowski, 1987; Bell et al., 1996), it is likely that soil bacteria attacks bone over a longer timescale when bones are buried, especially given that organics (i.e., collagen) can survive for millennia. It has been shown that microbial extracellular enzyme activity for carbon cycling enzymes significantly increases in soil closer to the surface (Upton et al., 2019). Thus, the pig legs in this experiment, lying on and partially submerged in the soil, were arguably exposed to more soil

450 microorganisms than if they would have been buried. Although the types of soil bacteria are
451 environment-specific such that the bioerosion features might manifest differently at various
452 locations, a large-scale study carried out by Brönnimann et al. (2018) did not find any
453 relationship between sediment type and intensity of microbial bioerosion.

454 Previous studies found that the first microscopic changes due to burning appear at
455 varying temperatures ranging from 600-1200°C. It is unknown where these temperatures
456 were measured (bone or air in furnace). In this study maximum mean bone temperatures
457 reached ≤750°C, while fire temperatures were as high as 995°C. If burnt and unburnt bone
458 microstructure is indeed indistinguishable at these temperatures, it is possible that these
459 subtle microscopic changes (e.g. 'Wedl 2' and 'MFD') caused by burning are mistaken for
460 bioerosion features. In general, the presence/absence of features on unburnt bones was less
461 variable than on burnt bones, meaning not all the bones are affected the same way by fire.
462 Variations might be due to the movement of the wind, flame height, soft tissue coverage, and
463 this variation might not be present when bones are burnt in a furnace. Thus, it is argued here
464 that experiments conducted on an outdoor fire give a better indication of real-life conditions
465 in both forensic and archaeological cases than bones burnt in a furnace.

466 Squires et al. (2011) noted that bones cremated at temperatures between 600-900°C
467 should have very few, if any, Volkmann's canals surviving. Conversely, it is argued here that
468 Volkmann's canals do survive 'intense cremation', as they were observed on all burnt bones.
469 They were recorded on 3.5% of fresh, unburnt samples, giving an indication of their expected
470 frequency. The fact that the bones were deposited in a terrestrial context – and hence not
471 exposed to cyanobacteria – further suggests that these features are mostly Volkmann's canals,
472 which can assume a variety of forms depending on the angles at which the bone is sectioned,
473 and so may be responsible for this discrepancy.

474 Hairline cracks are most probably due to the contraction and expansion of bone
475 attributable to weather changes, explaining the feature's positive correlation with longer
476 decay times in the unburnt groups, which disappeared post-burning. Cracks are considered to
477 be indications of collagen degradation (Huisman et al., 2017), but no statistically significant
478 increase was observed with time of deposition. Neither feature appears to be a useful
479 indicator for degradation in the bones, not least because the preparation of thin sections
480 and/or burning can cause them. The black enlarged lacunae and canaliculi may be present
481 because of carbon incorporation into the uneven surfaces of bone.

Demineralised and hypermineralised foci were sometimes present on the BSEM images of the unburnt bones. However, these foci did not resemble tunnels on BSEM images published by Fernández-Jalvo et al. (2010) and Turner-Walker (2019). Bright, heavily mineralised areas on the unburnt bones (e.g. Fig. 5) may instead relate to the structure of bone in young individuals, in which osteonal bone has not yet replaced the primary lamellar bone, producing a mixture of darker, less dense (younger) and heavier mineralised (older) areas (Boskey and Coleman, 2010), which can be mistaken for tunnelling. Hypermineralised areas with a less diffused degradation pattern than has been previously documented (Turner-Walker and Syversen 2002; Turner-Walker and Peacock 2008) suggest early bacterial bioerosion in some of the 3-months postmortem unburnt bones. All bioerosion-like features were obliterated through the burning process (Fig. 10). Therefore, BSEM is not a useful technique for identification of bioerosion features on burnt bones.

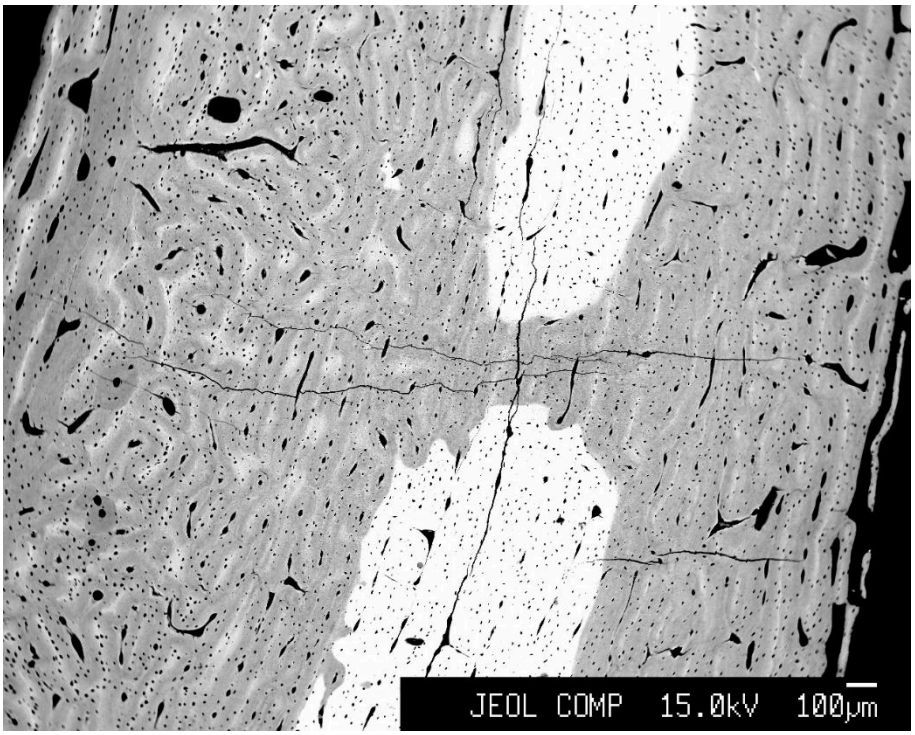

Fig. 10. Contrast differences due to burning of a 6-month decayed bone sample (WSF5D6M1_burnt). Note the central mineralised areas. (Electron microprobe, backscatter electron detector image.)

This study was conducted simultaneously with another recent study by Lemmers et al. (2020), with similar overall aims and methods. Although they suggest that bioerosion lesions have the potential to act as a proxy for the pre-burnt condition of the body, the opposite is

suggested here. The cause of this discrepancy might be that in the current study fresh, fleshed tibiae were burnt as controls, while the freshest bones in Lemmers et al.'s (2020) study were >3 years postmortem and may have been embalmed with a decomposition accelerator compound. In our study features indistinguishable from bioerosional features as described in the literature appeared on the fresh burnt controls, suggesting that they were produced by burning.

Limitations of the present study include the use of pigs as a proxy for humans and their young age (18 months), which might make them more susceptible to bioerosion due to the higher amount of organic matter in the bones. The data from the 1-year postmortem group are based on two samples, because the rest were removed by scavengers during the exposure phase. It was not possible to get access to a microtome, so thin sections were cut with a Buehler saw, producing a less consistent thickness across samples. All labelling was executed by one researcher (EIV) and due to the sheer number of blocks (N=27,000) some may have been incorrectly labelled. Balanced against this is the consistency in approach to identification that this permitted. Finally, the bones were not exposed to endogenous bioerosion, which should be the focus of future studies.

Conclusions

This study aimed to establish the utility of diagenetic features as a proxy for the body's state of decomposition prior to incineration. Ours is the first histotaphonomic study to apply a data labelling application, built for this purpose, to statistically assess bioerosion. We highlight the inconsistency in the literature concerning the naming of diagenetic features and their considered aetiologies. Although most recent literature is concerned with what the source of bacteria is (i.e. endogenous or exogenous), verification of which of these features are in fact caused by microbial bioerosion is more urgent. Our results showed that Wedl tunnelling, Wedl 2, and lamellate MFD are not reliable indicators of decomposition because similar features appear on freshly burnt bones, and thus can be caused by other factors, such as burning. Budded MFD was the only feature that showed a statistically significant increase in bone areas affected on both the unburnt and burnt groups. However, burning considerably reduced the visibility of this feature. Features labelled here as similar to 'cyanobacterial tunnelling' were in fact probably Volkmann's canals, which survived cremation on all bones. Hairline cracks did not appear to be informative on decay. Although BSEM is a useful tool in

bioerosion studies in unburnt bones, it cannot be used on burnt bones. In summary, it can be argued that microbial bioerosion features are not accurate proxies for the body's pre-burning condition and caution should be practised when identifying these in bones in both forensic and archaeological contexts.

Acknowledgements

The study was supported by the Meyerstein Foundation, School of Archaeology, University of Oxford. We would like to thank Prof. Robert Hedges for his insights into the study and Dr Victoria Smith for her help on the electron microprobe. We would also like to thank Mr Kevin Lemagnen for his help and support while developing the data labelling application. We thank the anonymous reviewers for their careful reading, valuable comments, and improvements made to the paper.

Funding

This work was supported by the Meyerstein Foundation, School of Archaeology, University of Oxford.

References

Absolonova, K., Veleminsky, P., Dobisikova, M., Beran, M., and Zocova, J. (2013). Histological estimation of age at death from the compact bone of burned and unburned human ribs. Journal of Forensic Sciences, 58, S135-S145.

Baby, R. S. (1954). Hopewell cremation practices. Papers in Archaeology. Ohio Historical Society, 1–7.

Bell, L. S. (2012a). Histotaphonomy. In C. Crowder and S. Stout (Eds.), Bone Histology: An Anthropological Perspective (pp. 241–251). Boca Raton, FL: Taylor and Francis.

Bell, L. S. (2012b). Identifying postmortem microstructural change to skeletal and dental tissues using backscattered electron imaging. In Lynne S. Bell (Ed.), Forensic Microscopy for Skeletal Tissues (pp. 173–190). Humana Press.

Bell, L. S., Boyde, A., Jones, S. J., and Bell, L. S. (1991). Diagenetic alteration to teeth in situ illustrated by backscattered electron imaging, 13, 173–183.

Bell, L. S., Skinner, M. F., and Jones, S. J. (1996). The speed of post mortem change to the human skeleton and its taphonomic significance. Forensic Science International, 82(2), 129–140.

Binford, L. R. (1963). An analysis of cremations from three Michigan sites. Wisconsin Archaeologist, 44, 98–110.

Boaks, A., Siwek, D., and Mortazavi, F. (2014). The temporal degradation of bone collagen: A histochemical approach. Forensic Science International, 240, 104-110.

Bonney, H., Colston, B., and Goodman, A. (2011). Regional variation in the mechanical properties of cortical bone from the porcine femur. Medical Engineering and Physics, 33(4), 513-520.

Bontrager, A. B., and Nawrocki, S. P. (2008). Cremains from the Fox Hollow Farm serial homicide site. In: Schmidt C. W., Symes S. A., editors. The Analysis of Burned Human Remains. London: Academic Press; 2008, 211–226.

Booth, T. J., and Madgwick, R. (2016). New evidence for diverse secondary burial practices in Iron Age Britain: A histological case study. Journal of Archaeological Science, 67, 14– 24.

Boskey, A. L., and Coleman, R. (2010). Critical reviews in oral biology and medicine: Aging and bone. Journal of Dental Research, 89(12), 1333–1348. https://doi.org/10.1177/0022034510377791

Bradtmiller, B., and Buikstra, J. E. (1984). Effects of burning on human bone microstructure: a preliminary study. Journal of Forensic Sciences, 29(2), 535–540.

Brönnimann, D., Portmann, C., Pichler, S. L., Booth, T. J., Röder, B., Vach, W., … Rentzel, P. (2018). Contextualising the dead – Combining geoarchaeology and osteoanthropology in a new multi-focus approach in bone histotaphonomy. Journal of Archaeological Science, 98(August), 45–58.

Buikstra, J. E., and Swegle, M. (1989). Bone modification due to burning: experimental evidence. In Bonnichsen, R. and Sorg, M. (Eds.), Bone Modification, College Station, TX: The Centre for the Study of the First Americans, 247–258.

Cambra-Moo, O., Barroso Bermejo, R., García Gil, O., Bueno Ramírez, P., Rascón Pérez, J., González Martín, A., … Rietveld, H. M. (2017). The effect of soft tissue on temperature estimation from burnt bone using Fourier Transform Infrared Spectroscopy. Journal of Forensic Sciences, 35(1), 1–8.

Carroll, E. L., and Kirsty E. Squires. "Burning by Numbers: A Pilot Study Using Quantitative Petrography in the Analysis of Heat-induced Alteration in Burned Bone." International Journal of Osteoarchaeology 30.5 (2020): 691-99. Web.

Castillo, F., Ubelaker, D. H., Acosta, J. A., de la Rosa, R. J., and Garcia, I. G. (2013). Effect of temperature on bone tissue: Histological changes. Journal of Forensic Sciences, 58(3), 578–582. https://doi.org/10.1111/1556-4029.12093

Cattaneo, C., DiMartino, S., Scali, S., Craig, O. E., Grandi, M., and Sokol, R. J. (1999). Determining the human origin of fragments of burnt bone: A comparative study of histological, immunological and DNA techniques. Forensic Science International, 102(2–3), 181–191.

603 Child, A. (1995). Towards and Understanding of the Microbial Decomposition of
604 Archaeological Bone in the Burial Environment. Journal of Archaeological Science, 22(2),
605 165-174.

606 Cooney, G., Quinn, C., P., Kuijt, Ian (2014). Transformation by fire. Tucson : University of
607 Arizona Press.

608 Collins, M. J., Nielsen–Marsh, C. M., Hiller, J., Smith, C. I., Roberts, J. P., Prigodich, R. V., …
609 Turner–Walker, G. (2002). The survival of organic matter in bone: a review. Archaeometry.
610 44(3), 383-394.

611 Daniel, J. C., and Chin, K. (2010). The role of bacterially mediated precipitation in the
612 permineralization of bone. PALAIOS. SEPM (Society for Sedimentary Geology). 25(7/8), 507-
613 516.

614 Dowd, M. A. (2008). The use of caves for funerary and ritual practices in Neolithic Ireland.
615 Antiquity, 82, 305–317.

616 Etxeberria, F. (1994). Aspectos macroscópicos del hueso sometido al fuego: revisión de las
617 cremaciones descritas en el País Vasco desde la arqueologia. Munibe, 46, 111–116.

618 Fairgrieve, S. I. (2008). Forensic Cremation Recovery and Analysis. Boca Raton, FL: CRC Press.
619 Farmer, A. (1995). Soil chemistry change in a lowland english deciduous Woodland 1974–
620 1991. Water, Air, and Soil Pollution. 85(2), 677-682.

621 Farmer, A. (1995). Soil chemistry change in a lowland english deciduous Woodland 1974–
622 1991 [Article]. In Water, Air, and Soil Pollution (Vol. 85, Issue 2, pp. 677–682). Kluwer
623 Academic Publishers. https://doi.org/10.1007/BF00476907

624 Feng, L., and Jasiuk, I. (2011). Multi-scale characterization of swine femoral cortical bone.
625 Journal of Biomechanics, 44(2), 313-320.

626 Fernández-Jalvo, Y., Andrews, P., Pesquero, D., Smith, C., Marín-monfort, D., Sánchez, B., …
627 Alonso, A. (2010). Early bone diagenesis in temperate environments Part I : Surface features
628 and histology. Palaeogeography, Palaeoclimatology, Palaeoecology, 288(1–4), 62–81.

629 Forbes, S. L., Stuart, B. H., and Dent, B. B. (2005). The effect of the method of burial on
630 adipocere formation. Forensic Science International, 154(1), 44-52.

631 Garland, A. N. (1987) A histological study of archaeological bone decomposition.
632 Boddington, A., Garland, A. N., Janaway, R. C. (Eds.), Death, Decay, and Reconstruction:
633 Approaches to Archaeology and Forensic Science. Manchester University Press, Manchester,
634 109– 126.

635 Garrido-Varas, C., and Intriago-Leiva, M. (2015). The interpretation and reconstruction of
636 the post-mortem events in a case of scattered burned remains in Chile. In T. Thompson
637 (Ed.), The Archaeology of Cremation: burned human remains in funerary studies.
638 Havertown: Oxbow Books, 227-242.

639 Gonçalves, D., Thompson, T. J. U., and Cunha, E. (2011). Implications of heat-induced
640 changes in bone on the interpretation of funerary behaviour and practice. Journal of
641 Archaeological Science, 38(6), 1308–1313.

642 Grévin, G., Baud, C., and Susini, A. (1991). Etude anthropologique et paléopathologique d ’
643 un adulte inhumé puis incinéré provenant du site de Pincevent (Seine-et-Marne), Bulletins
644 et Mémoires de la Société d'Anthropologie de Paris 2(3-4), 77–87.

645 Grine, F. E., Bromage, T. G., Daegling, D. J., Burr, D. B., and Brain, C. K. (2015). Microbial
646 osteolysis in an Early Pleistocene hominin (Paranthropus robustus) from Swartkrans , South
647 Africa. Journal of Human Evolution, 85, 126–135.

648 Hackett C.J. (1981). Microscopial Focal Destruction (Tunnels) in Exhumed Human Bones.
649 Medicine, Science and the Law, 21(4), 243–265.

650 Hedges, R. E. M., and Millard, A. R. (1995). Bones and Groundwater: Towards the Modelling
651 of Diagenetic Processes. Journal of Archaeological Science 22/ 2, 155–164.
652 https://doi.org/10.1006/jasc.1995.0017

653 Hedges, R.E.M., Millard, A.R., Pike, A.W.G., (1995). Measurements and relationships of
654 diagenetic alteration of bone from three archaeological sites. Journal of Archaeological
655 Science, 22, 201-209. https://doi.org/10.1006/jasc.1995.0022

656 Herrmann, B. (1976). Neuere Ergebnisse zur Beurteilung menschilcher Brandknochen. Z.
657 Rechtsmedizin, 17, 191–200.

658 Herrmann, B. (1977). On histological investigations of cremated human remains. Journal of
659 Human Evolution, .6(2), 101-103.

660 Holden, J., Phakey, P., and Clement, J. (1995). Scanning electron microscope observations of
661 heat-treated human bone. Forensic Science International, 74(1-2), 29-45.

662 Holden, J. L., Clement, J. G., and Phakey, P. P. (1995). Age and temperature related changes
663 to the ultrastructure and composition of human bone mineral. Journal of Bone and Mineral
664 Research, 10(9), 1400-1409.

665 Hollund, H. I., Jans, M. M. E., Collins, M. J., Kars, H., Joosten, I., and Kars, S. M. (2012). What
666 Happened Here? Bone Histology as a Tool in Decoding the Postmortem Histories of
667 Archaeological Bone from Castricum, The Netherlands. International Journal of
668 Osteoarchaeology, 22(5), 537-548.

669 Hollund, Hege I, Jans, M. M. E., and Kars, H. (2014). How are teeth better than bone? An
670 investigation of dental tissue diagenesis and state of preservation at a histological scale
671 (with photo catalogue). Internet Archaeology 36.

672 Huisman, D.J., Raemaekers, D.C.M., Jongmans, A.G. (2009). Investigating Early Neolithic land
673 use in Swifterbant (NL) using micromorphological techniques. Catena 78(3), 185e197.

674 Huisman, H., Ismail-Meyer, K., Sageidet, B. M., and Joosten, I. (2017). Micromorphological
675 indicators for degradation processes in archaeological bone from temperate European
676 wetland sites. Journal of Archaeological Science, 85, 13-29.

677 Hummel, S., and Schutkowski, H. (1986). Bedeutungen für die Leichenbranddiagnose. Mit 4
678 Abbildungen und 1 Tabelle im Text. Zeitschrift für Morphologie und Anthropologie, 77(1), 1-
679 9.

680 Imaizumi, K., Taniguchi, K., and Ogawa, Y. (2014). DNA survival and physical and histological
681 properties of heat-induced alterations in burnt bones. International Journal of Legal
682 Medicine, 128(3), 439-446.

683 Jans, M. M.E., Nielsen-Marsh, C. M., Smith, C. I., Collins, M. J., and Kars, H. (2004).
684 Characterisation of microbial attack on archaeological bone. Journal of Archaeological
685 Science, 31(1), 87–95.

686 Jans, M. M. E, Kars, H., Nielsen-Marsh, C. M., Smith, C. I., Nord, A. G., Arthur, P., and Earl, N.
687 (2002). in Situ Preservation of Archaeological Bone: a Histological Study Within a
688 Multidisciplinary Approach. Archaeometry, 44, 343–352.

689 Jans, M. M. E. (2005). Histological Characterisation of Diagenetic Alteration of
690 Archaeological Bone. (Unpublished doctoral dissertation) Amsterdam: Institute for Geo and
691 Bioarchaeology.

692 Jans, M. M. E. (2008). Microbial bioerosion of bone - a review. In Wisshak, M. and Tapanila,
693 L. (Eds.), Current Developments in Bioerosion. Berlin, Heidelberg: Springer, 397-493.

694 Jans, M. M E. (2013). Microscopic destruction of bone. In J. T. Pokines and S. A. Symes (Eds.),
695 Manual of Forensic Taphonomy, CRC Press, Taylor and Francis group, 19-35.

696 Kendall, C., Marie, A., Eriksen, H., Collins, M. J., Turner-Walker, G., and Kontopoulos, I.
697 (2018). Diagenesis of archaeological bone and tooth. Palaeogeography, Palaeoclimatology,
698 Palaeoecology, 491(November 2017), 21–37.

699 Kontopoulos, I. (2019). Bone diagenesis in a Mycenaean secondary burial (Kastrouli,
700 Greece), Archaeological and Anthropological Sciences, 11, 5213–5230.

701 Kontopoulos, I., Nystrom, P., and White, L. (2016). Experimental taphonomy : post-mortem
702 microstructural modifications in sus scrofa domesticus bone. Forensic Science International,
703 266(April 2019), 320–328.

704 Lemmers, S. A. M., Gonçalves, Cunha, E., D., Vassalo, A., R., and Appleby, J. (2020). Burned
705 Fleshed or Dry ? The Potential of Bioerosion to Determine the Pre-Burning Condition of
706 Human Remains. Journal of Archaeological Method and Theory.

707 Lynn, K. S., and Fairgrieve, S. I. (2009). Microscopic Indicators of Axe and Hatchet Trauma in
708 Fleshed and Defleshed Mammalian Long Bones. Journal of Forensic Sciences, 54(4), 793–
709 797.

Millard, A. (1993). Diagenesis of archaeological bone: the case of uranium uptake. (Unpublished doctoral thesis) University of Oxford: Research Laboratory for Archaeology and the History of Art.

Millard, A. R. (2001). Deterioration of Bone. In D. R. Brothwell and A. M. Pollard (Eds.), Handbook of Archaeological Sciences. Chichester ; New York : J. Wiley, 637-647.

Morales, N. S., Catella, L., Oliva, F., Sarmiento, P. L., and Barrientos, G. (2018). Journal of Archaeological Science: Reports. A SEM-based assessment of bioerosion in Late Holocene faunal bone assemblages from the southern Pampas of Argentina. Journal of Archaeological Science: Reports, 18, 782–791.

Nelson, R. (1992). A Microscopic Comparison of Fresh and Burned Bone. Journal of Forensic Sciences, 37(4), 1055–1060.

Nicholson, R. A. (1993). A morphological investigation of burnt animal bone and an evaluation of its utility in archaeology. Journal of Archaeological Science, 20(4), 411- 428.

Nielsen-Marsh, C. M., and Hedges, R. E. . (2002). Patterns of Diagenesis in Bone I: The Effects of Site Environments. Journal of Archaeological Science, 27(12), 1139–1150.

Nielsen-Marsh, C. M., Smith, C. I., Jans, M. M. E., Nord, A., Kars, H., and Collins, M. J. (2007). Bone diagenesis in the European Holocene II : taphonomic and environmental considerations. Journal of Archaeological Science, 34(9), 1523-1531.

Pearce, A. I., Richards, R. G., Milz, S., Schneider, E., and Pearce, S. G. (2007). Animal models for implant biomaterial research in bone: A review. European Cells and Materials, 13(0), 1–10. https://doi.org/10.22203/eCM.v013a01

Pechal, J. L., Tawni L Crippen, Aaron M Tarone, Andrew J Lewis, Jeffery K Tomberlin, and M Eric Benbow. (2013). Microbial community functional change during vertebrate carrion decomposition. PLoS ONE. 8(11), e79035.

Pesquero, M. D., Bell, L. S., Fernández-jalvo, Y., Pesquero, M. D., Bell, L. S., and Fernández-jalvo, Y. (2018). Skeletal modification by microorganisms and their environments. Historical Biology, 2963, 1–12. https://doi.org/10.1080/08912963.2017.1371713

Piepenbrink, H. (1986). Two examples of biogenous dead bone decomposition and their consequences for taphonomic interpretation. Journal of Archaeological Science, 13(5), 417-430.

Piepenbrink, H., and Schutkowski, H. (1987). Decomposition of skeletal remains in desert dry soil A roentgenological study. Human Evolution, 2(6), 481–491.

Quatrehomme, G., Bolla, M., Muller, M., Rocca, J., Grévin, G., Bailet, P., and Ollier, A. (1998). Experimental Single Controlled Study of Burned Bones: Contribution of Scanning Electron Microscopy. Journal of Forensic Sciences, 43(2), 417–422.

Roux, G. A. D. T. (1887). Contribution à l'étude clinique et thérapeutique des taenias de l'homme. (Unpublished doctoral thesis) University of Lyon, Lyon, France.

747 Spennemann, D. H. R., Colley, S. M. (1989). Fire in a Pit: the effects of burning on faunal
748 remains. Archaeozoologia, 3, 51–64.

749 Squires, K. E., Thompson, T. J. U., Islam, M., and Chamberlain, A. (2011). The application of
750 histomorphometry and Fourier Transform Infrared Spectroscopy to the analysis of early
751 Anglo-Saxon burned bone. Journal of Archaeological Science, 38(9), 2399–2409.

752 Symes, A., S., Dirkmaat, D. C., Ousley, S., Chapman, E., Cabo, L. (2012) Recovery and
753 Interpretation of Burned Human Remains. NIJ Report. National Institute of Justice Available
754 at https://www.ncjrs.gov/pdffiles1/nij/grants/237966.pdf (20/04/2016).

755 Taylor, M. E., Morecroft, M. D., and Oliver, H. R. (2011). The Physical Environment. Wytham
756 Woods. Oxford University Press.

757 Thompson, T. J. U., and Inglis, J. (2009). Differentiation of serrated and non-serrated blades
758 from stab marks in bone. International Journal of Legal Medicine, 123(2), 129–135.

759 Tjelldén, A. K. E., Kristiansen, S. M., Birkedal, H., and Jans, M. M. E. (2018). The pattern of
760 human bone dissolution—A histological study of Iron Age warriors from a Danish wetland
761 site. International Journal of Osteoarchaeology, 28(4), 407–418.

762 Trueman, C. N., and Martill, D. M. (2002). The long–term survival of bone: the role of
763 bioerosion. Archaeometry. 44(3), 371-382.

764 Turner, B., and Wiltshire, P. (1999). Experimental validation of forensic evidence : a study of
765 the decomposition of buried pigs in a heavy clay soil, Forensic Science International 101,
766 113–122.

767 Turner-Walker, G. (2012). Early bioerosion in skeletal tissues : Persistence through deep
768 time Early bioerosion in skeletal tissues: persistence through deep time, Neues Jahrbuch für
769 Geologie und Paläontologie - Abhandlungen 265(2), 165-183.

770 Turner-Walker, G. (2014). The Chemical and Microbial Degradation of Bones and Teeth. In:
771 Pinhasi, R. and Mays, S. (Eds.) Advances in Human Palaeopathology. John Wiley and Sons, 3-
772 29.

773 Turner-Walker, G. (2019). Light at the end of the tunnels ? The origins of microbial
774 bioerosion in mineralised collagen. Palaeogeography, Palaeoclimatology, Palaeoecology,
775 529, 24–38.

776 Turner-Walker, G. and Syversen, U. (2002). Quantifying histological changes in
777 archaeological bones using BSE-SEM image analysis. Archaeometry, 44(3), 461-468.

778 Turner-Walker, G. and Jans, M. (2008). Reconstructing taphonomic histories using
779 histological analysis. Palaeogeography, Palaeoclimatology, Palaeoecology, 266(3), 227-235.

780 Turner-Walker, G. and Peacock, E.E. (2008). Preliminary results of bone diagenesis in
781 Scandinavian bogs. Palaeogeography, Palaeoclimatology, Palaeoecology, 266(3-4), 151-159.

782 Ubelaker, D. H. (2009). The forensic evaluation of burned skeletal remains: A synthesis.
783 Forensic Science International, 183(1–3), 1–5.

784 Upton, R. N., A. Checinska Sielaff, K. S. Hofmockel, X. Xu, H. W. Polley, and B. J. Wilsey. 2019.
785 Soil depth and grassland origin cooperatively shape microbial community cooccurrence and
786 function. Ecosphere 11(1):e02973.

787 Van Vark, G. N. (1970). Some Statistical Procedures for the Investigation of Prehistoric
788 Human Skeletal Material. Groningen: Rijksuniversiteir te Groningen.

789 Waterman, D. M. (1978) The Excavation of a Court Cairn at Tully, Co. Fermanagh. Ulster
790 Journal of Archaeology 41, 3–14.

791 Wedl, C. (1864). Über einen im Zahnbein und Knochen keimenden Pilz. Sitzungsberichte Der
792 Kaiserlichen Akademie Der Wissenschaften Zu Wien, Mathematisch- Naturwissenschaftliche
793 Classe, 50(1), 171–193.

794 Wells, C. (1978). Notes on Cremated Bones from Tully Court Cairn. Ulster Journal of
795 Archaeology, 41, 13–14.

796 White, L., and Booth, T. J. (2014). The origin of bacteria responsible for bioerosion to the
797 internal bone microstructure: Results from experimentally-deposited pig carcasses. Forensic
798 Science International, 239, 92–102.

799 Whyte, T. (2001). Distinguishing remains of human cremations from burned animal bones.
800 Journal of Field Archaeology, 28, 437–448.

801 Wilson, A. S., Janaway, R. C., Holland, A. D., Dodson, H. I., Baran, E., Pollard, A. M., Desmond,
802 T. J. (2007). Modelling the buried human body environment in upland climes using three
803 contrasting field sites. Forensic Science International, 169, 6–18.

804 Yoshino, M., Kimijima, T., Miyasaka, S., Sato, H., and Seta, S. (1991). Microscopical study on
805 estimation of time since death in skeletal remains. Forensic Science International, 49(2),
806 143-158. https://doi.org/10.1016/0379-0738(91)90074-S.